Article:
Liu, Y., Fu, C., Li, Y. et al. (3 more authors) (2025) Uncovering hidden dangers in urban housing: Sources of indoor radon and associated health risks. Journal of Environmental Management, 387. 125899. ISSN: 0301-4797

https://doi.org/10.1016/j.jenvman.2025.125899

Uncovering Hidden Dangers in Urban Housing: Sources of Indoor Radon and Associated Health Risks

Abstract

Radon, a naturally occurring radioactive gas, tends to accumulate indoors and can reach hazardous concentrations that pose significant health risks. Globally, radon is recognized as the second leading cause of lung cancer after smoking. Despite its well-documented dangers, significant knowledge gaps persist regarding the sources of radon exposure and the resulting health risks. In this study, we examine the spatial and temporal distribution, sources, and health impacts of indoor radon in Ohio, USA—a state characterized by diverse geological and meteorological conditions and radon concentrations significantly exceeding the national average, contributing to approximately 900 lung cancer deaths annually. Our results reveal pronounced spatial heterogeneity, with elevated radon concentrations in central urban areas, and seasonal variability, with higher levels during winter. Using statistical analysis and structural equation modeling, we identify surface radiation sources, meteorological conditions, and building materials as key drivers of indoor radon accumulation. Furthermore, Monte Carlo simulations indicate that the estimated lifetime excess cancer risk for residents in the study area is 2.29%, approximately double the standard safety threshold. These findings underscore the urgent need to raise awareness of radon-induced carcinogenesis and to implement effective mitigation strategies to safeguard public health.

Keywords: Indoor radon; Structural equation modeling; Source apportionment; Risk assessment; Ohio

1. Introduction

Radon is an odorless, colorless, and chemically inert radioactive gas that typically exists in the form of various radioisotopes (Nayak et al., 2022; Takahashi et al., 2022). Among the 27 known radon isotopes, ^{222}Rn is the most significant in terms of human health, accounting for approximately 80% of all radon-related exposure (Kim et al., 2024). By interacting with biomolecules in the lungs, radon can cause large-scale molecular changes and deposit decay products in the lungs, thereby increasing the risk of cancer (Robertson et al., 2013; Somsunun et al., 2022). Consequently, radon is recognized as the second leading cause of lung cancer worldwide, trailing only behind smoking, with an estimated 3-20% of global lung cancer fatalities attributed to radon exposure (Azhdarpoor et al., 2021; Forouzanfar et al., 2015; Kalankesh et al., 2024; Liu et al., 2024a; Madas et al., 2022).

Radon gas diffuses and decays naturally in the air, but accumulates and eventually builds up to dangerous levels in poorly ventilated indoor environments, such as homes, offices, and schools, which are the main sites of radon exposure. Epidemiological studies have consistently demonstrated a clear link between indoor radon exposure and an increased risk of lung cancer. Specifically, a 100 Bq/m³ increase in indoor radon concentration (IRC) is associated with an 8%-16% rise in lung cancer risk (Forouzanfar et al., 2015; Su et al., 2022a; Turner et al., 2011). Notably, a positive correlation between radon concentration and relative risk becomes particularly evident when indoor levels exceed 200 Bq/m³ (Xue et al., 2022). For example, a study in Ireland found that individuals residing in areas with radon concentrations exceeding 200 Bq/m³ were 2.9 to 3.1 times more likely to develop lung cancer compared to those living in areas with lower concentrations (Deinpsey et al., 2018). In response to this public health threat**,** various national and international health agencies have issued radon exposure guidelines. The International Commission on Radiological Protection (ICRP) recommends that indoor radon levels not exceed 300 Bq/m³, while outdoor workplace levels should remain below 1000 Bq/m³ (Lecomte et al., 2014). Similarly, various countries have implemented regulations to limit indoor radon exposure, with reference levels set at 300 Bq/m³ in Spain, 250 Bq/m³ in Germany, 200 Bq/m³ in the United Kingdom, and 148 Bq/m³ in the United States, as per the Environmental Protection Agency (EPA) guidelines (Lecomte et al., 2014; Liu et al., 2024b).

Understanding the variation in indoor radon levels requires identifying its primary sources and the factors that influence its movement and accumulation. Major sources of indoor radon include soil, domestic water, building materials, nearby fuels, and the infiltration of outdoor radon. These sources are affected by meteorological conditions, ventilation strategies, and human lifestyle choices (Carrion-Matta et al., 2021; Casey et al., 2015; Kellenbenz and Shakya, 2021; Li et al., 2021; Li et al., 2023a; Liu et al., 2024b; Seyis et al., 2022). Collectively, these influences can be grouped into four broad categories: geological, building-related, meteorological, and socio-economic factors. Geological factors are pivotal in controlling the production of radon and its ability to diffuse through the ground. Radon is produced through the radioactive decay of uranium and thorium in the earth's crust, with uranium content in ores and sedimentary rocks, such as shale, sandstone, and limestone, directly influencing IRC in a given region (Rodriguez-Martinez et al., 2018). Additionally, the physical and chemical properties of soil, including porosity and permeability, significantly affect the migration and release of radon from underground sources into the indoor environment (Riudavets et al., 2022). Building factors are equally crucial in radon

infiltration. Construction materials and building usage patterns influence how efficiently radon is released from surfaces and accumulates in indoor air (Ajrouche et al., 2017). The structure and design of a building, including its foundation type and ventilation systems, directly impact the frequency of radon exposure and the effectiveness of indoor air circulation (Tung et al., 2013). Furthermore, building density can indicate household water sources and associated radon risk: higher-density areas are typically served by municipal supplies with lower radon levels, while lower-density areas often rely on private wells, which tend to have higher concentrations (Li et al., 2023a).

Meteorological conditions significantly affect radon release and dispersion. Factors such as precipitation, surface temperature, air pressure, snow depth, and soil moisture influence both radon migration from the subsurface and its concentration in outdoor air (Chaudhuri et al., 2010; Xie et al., 2015). Seasonal variations in indoor radon levels are largely driven by meteorological factors. In winter, warmer indoor temperatures generate a pressure gradient that drives radon-laden soil gases into buildings. Limited ventilation during this period further increases indoor radon levels (Schubert et al., 2018). Socio-economic factors also play a role by influencing energy efficiency and the adoption of radon mitigation measures. Interestingly, a study conducted in the UK found that radon exposure was more strongly associated with higher socio-economic status households, where radon levels were, on average, higher than in lower socio-economic households; the latter had approximately two-thirds the radon concentration of their wealthier counterparts (Kendall et al., 2016).

Despite the well-established influence of these factors, there is still a lack of comprehensive studies that explore their complex interactions in the context of specific geographic regions, highlighting a critical gap in current radon research. In particular, the synergistic effects of geological and anthropogenic factors on radon levels remain underexplored. This study addresses these knowledge gaps by focusing on the U.S. state of Ohio, which presents a unique and compelling case due to its uranium-rich geology and consistently elevated radon concentrations. Ohio's organic shales and uranium-bearing soils contain high concentrations of uranium (10-40 ppm), which are 5 to 20 times higher than average crustal concentrations (Kumar et al., 2011; Li et al., 2023b). When the uranium decays, it forms radon that enters homes through soil, underground water, and water distribution systems, and, in a gaseous form, through cracks and other openings (Manawi et al., 2024). The United States Environmental Protection Agency (USEPA) has classified Ohio as a Zone 1 state (i.e., mean indoor radon screening levels greater than 4 pCi/L) (Gummadi et al., 2015; Poku and Hussaini, 2024). Alarmingly, an estimated 700 to 1,300 annual lung cancer deaths in Ohio are attributed to radon exposure, representing about 5% of the national total (Acree et al., 2017; Hahn et al., 2020; Kumar et al., 2010).

In summary, this study has three primary objectives: (1) to characterize the spatial and temporal variability of indoor radon concentrations (IRC) in Ohio, (2) to identify the environmental factors driving this variability, and (3) to evaluate the potential health risks associated with indoor radon exposure. By analyzing the complex interactions among environmental, structural, and socio-economic factors, this research aims to inform targeted mitigation strategies and ultimately reduce radon-related health risks in Ohio and other similarly affected regions. The findings are expected to enhance the understanding of indoor radon dynamics in high-risk areas and support the development of evidence-based public health interventions.

2. Materials and methods

2.1. Study area description

Ohio (38°25'27"~42°15'37"N, 80°31'37"~84°49'27"W) is situated in the east-central United States, within the Great Lakes region, and spans a total area of 116,096 km² (Figure 1). Topographically, Ohio consists mainly of plains and hills, with low mountain ranges in the east, and relatively flat terrain, with an elevation of 143~456 meters above sea level. The climate is temperate continental. The average precipitation in the region is 800~1000 mm, with precipitation mainly concentrated in spring and summer, annual evaporation is 1200 mm, and the average annual temperature is 11.5 °C. Geologically, the state is composed predominantly of sedimentary, metamorphic, and igneous rocks, and is rich in mineral resources such as coal, limestone, and sandstone. Notably, Ohio lies along the West Ohio Seismic Zone and partly within the Southern Great Lakes Seismic Zone, resulting in numerous subsurface fault lines.

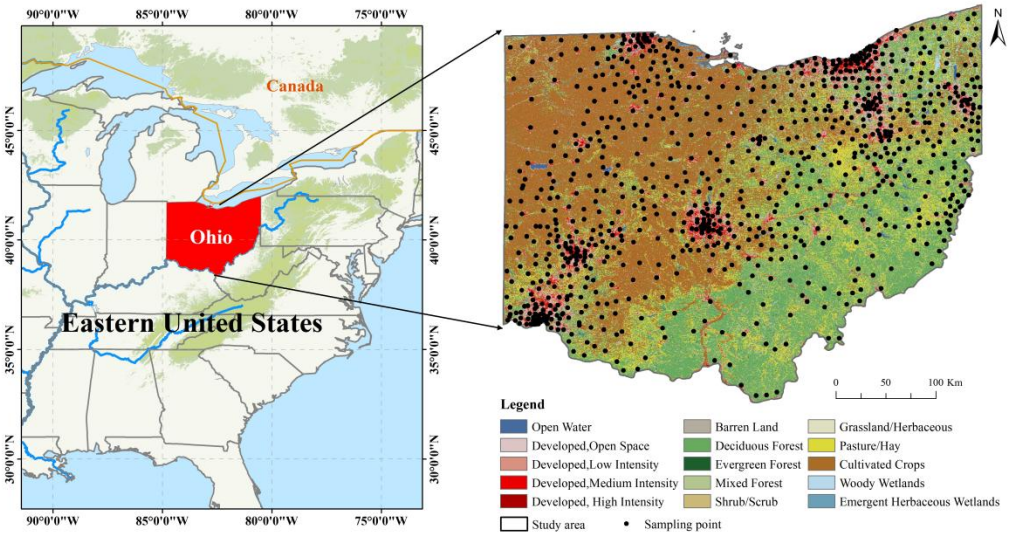

Fig. 1 Study area and indoor radon sampling locations (n=935)

2.2. Data collection and processing

Data on radon gas concentrations in homes were obtained from the Ohio Department of Health. This study utilized residential radon measurement data collected from 2007 to 2015, totaling 149,163 records, and the spatial distribution of 935 sampling points is shown in Figure 1. The dataset included information on radon concentration, geographic coordinates (longitude and latitude), seasonal codes, and year of measurement. To avoid masking effects during model training, we excluded measurements exceeding 20 pCi/L (95th percentile), which accounted for 5,598 records (Chen and Bill, 1983).

We categorized the factors influencing IRC into four main groups: geological, building, meteorological, and socioeconomic factors (Li et al., 2021; Li et al., 2023a). Geologic factors control radon production, emission, and subsurface movement, including ground surface concentration of uranium-238 (^{238}U) and thorium-232 (^{232}Th), lithology, sediments, geological era, gravity anomalies, and the distance to geological faults and mineral resources. Additionally, we

included soil parameters such as water availability capacity, organic matter percentage, saturated hydraulic conductivity, vertical permeability, bulk weight, field water holding capacity, porosity, erodibility, depth, and percentage composition of soil components of different grain sizes (gravel, sand, and clay). Building factors affect radon infiltration from the soil to the indoor environment. We included key building characteristics such as age, price, number of floors, ventilation systems (heating or cooling methods), energy use, building materials, roof structure, and water source. Meteorological factors affect the release of radon gas from the soil to the atmosphere, the movement of radon in the ground, and the atmospheric radon concentration, including precipitation, air temperature, water vapor pressure, evapotranspiration, snow water equivalent, and rapid runoff. Socioeconomic factors reflect human lifestyles and the prevalence of radon mitigation measures. We incorporated variables such as household income, education level, and household demographics.

Geological and soil data were obtained from the U.S. Geological Survey and the U.S. Department of Agriculture. Building information was extracted from the Realtor real estate website based on the location of the homes where radon samples were collected. Meteorological data were primarily sourced from the Daymet Version 4 dataset, and socioeconomic attributes of the study area were retrieved from the U.S. Census Grids data. All raster data were resampled to a consistent spatial resolution of 1 km × 1 km to ensure comparability across datasets. Detailed information on the environmental variables—including their names, abbreviations, categories, units, and data sources—is provided in the Supplementary Material (Table S1).

2.3. Statistical analysis

We conducted descriptive statistics, one-way analysis of variance (ANOVA), and Tukey's test for significant differences using IBM SPSS Statistics (version 25.0), considering differences significant at $P < 0.05$. To assess the relationships between IRC and numeric environmental factors, we employed Spearman's correlation, as it is a non-parametric method suitable for evaluating monotonic associations without assuming normal distribution of the data (Chen et al., 2024; Parveen et al., 2021). In addition, we applied the Geodetector method to investigate the spatial heterogeneity of IRC and to identify the driving forces behind it. Geodetector has been widely applied in environmental science, social science, and public health studies due to its ability to handle nonlinear relationships, its straightforward structure, and its clear interpretability (Liu et al., 2023; Wan and Shi, 2022; Wang et al., 2016). Specifically, we utilized the factor and divergence detection modules to quantify the explanatory power of categorical environmental factors on IRC variation. Furthermore, the risk zone detection module was applied to examine significant differences in mean IRC values across different subregions. To examine the direct and indirect effects of environmental factors on IRC and evaluate complex causal relationships, we applied Partial Least Squares Structural Equation Modeling (PLS-SEM) (Gu et al., 2022; Guo et al., 2021; Xie et al., 2022). 31 indicators were selected from a total of 46, and these were grouped into 15 latent variables based on correlation analysis results and goodness of fit (GOF), including geology, tectonics, geophysical features, soil composition, soil water, soil features, surface features, surface radiation, hydroclimate, building features, building materials, heating features, cooling features, domestic water, and socioeconomic and population factors. Spatial interpolation using ordinary kriging (OK) was used to identify the spatial structure of IRC and associated health risks across Ohio. Spearman's correlation and PLS-SEM were conducted using the "corrplot" and

"plspm" packages in R Statistical Software (version 4.2.2), respectively, while GIS mapping and spatial interpolation were performed using ArcMap 10.8. Statistical analysis charts were generated using Origin 2022. Detailed methodology and operational procedures are provided in the supplementary materials (Text S1–S3).

2.4. Health risk assessment

The average annual effective dose (E_{Rn}) (mSv/y) to occupants of Ohio homes from inhalation of indoor radon was estimated using the UNSCEAR-2000 model (Bulut and Sahin, 2023), based on measurements of the average annual IRC in the buildings:

$$E_{Rn} = C_{Rn} \times F \times H \times T \times D \quad (1)$$

where C_{Rn} is the IRC in Bq/m^3, converted by 1 pCi/L = 37 Bq/m^3. F is the equilibrium factor between radon and its short-lived daughters (0.4 for residential premises). H is the occupancy factor (0.8, defined as 80% of the interior space in the home). T is the annual time spent indoors (8760 h/y). D is the dose conversion factor (9 nSv/Bq m^{-3} h^{-1}). The formula is multiplied by 10^{-6} to convert the result to mSv/y.

The excess lifetime cancer risk (ELCR) is a potential carcinogenic effect that expresses the probability or risk of developing cancer in an individual exposed to a certain dose of radiation over a specific time period (Kalankesh et al., 2024). ELCR due to radon exposure is calculated using the following formula:

$$ELCR = E_{Rn} \times DL \times RF \quad (2)$$

where DL denotes mean life span (70 y), and RF is the risk factor, using the public exposure value (5.5 × 10^{-2} Sv^{-1}) recommended by ICRP 103.

Finally, the number of lung cancer cases (LCC) per million people per year was estimated using the following formula:

$$LCC = E_{Rn} \times RFLC \quad (3)$$

where $RFLC$ is an ICRP 50 reported (Smith, 1988) risk factor for lung cancer induction per million population of 18 × 10^{-6} mSv^{-1} y.

2.5. Monte Carlo simulation

Monte Carlo simulation (MCS) is a probabilistic method used to address uncertainty and has been employed to study uncertainty levels and conduct sensitivity analyses for risk sites (Gu et al., 2022). In assessing the health risk of indoor radon exposure, we used IRC values as assumptions and ELCR values as predictors, and conducted separate simulations for different age groups, smoking status and gender to generate probability distributions of individual cancer risk taking into account the exposure rate and risk factors specific to different population groups (Kalankesh et al., 2024). The simulations were conducted using Oracle Crystal Ball v11.1.24 (Oracle, USA), with 10,000 iterations performed to obtain plausible risk outputs. The detailed simulation process is described in the Supplementary Material (Text S4).

3. Results and discussion

3.1. Temporal-spatial variation and characterization of IRC in Ohio

3.1.1 Describe the statistical characteristics

The descriptive statistical characteristics and temporal variation of IRC are presented in Table 1 and Figure 2, A1-A3. The variation in the mean IRC values from 2007 to 2015 ranged from 4.13 to 5.03 pCi/L, with most values falling within the range of 1-10 pCi/L. According to the U.S. EPA's 1987 recommended reference level for IRC, only 59% (83,218/143,565) of the tested samples met this criterion, indicating that the installation of mitigation systems is necessary in most parts of the study area. Despite fluctuations in the annual mean IRC values over the study period, an overall upward trend was observed, becoming more pronounced when viewed at five-year intervals.

Table 1. Descriptive statistics for IRC from 2007 to 2015

Year	Points	Tests	Quantile		Median	Mean	SD	CV	Skewness	Kurtosis
			5%	95%						
2007	584	11320	0.95	9.30	3.49	4.13	2.87	0.70	1.91	5.52
2008	610	11633	1.00	10.38	3.75	4.43	3.08	0.70	1.63	3.60
2009	536	7919	1.20	11.30	4.4	5.03	3.20	0.64	1.31	2.17
2010	563	8153	1.20	10.99	4.1	4.89	3.18	0.65	1.41	2.67
2011	605	13730	1.10	10.00	3.80	4.46	2.89	0.65	1.57	3.74
2012	662	17381	1.23	10.40	4.34	4.90	2.94	0.60	1.26	2.43
2013	683	24789	1.10	9.19	3.90	4.36	2.64	0.61	1.71	4.96
2014	688	22893	1.30	9.90	4.13	4.70	2.78	0.59	1.46	3.45
2015	722	31345	1.30	9.70	4.10	4.59	2.73	0.60	1.63	4.31

3.1.2 Seasonal variations

ANOVA and Tukey's test showed a significant difference in IRC across the four seasons ($F = 142.04$, $P < 0.05$). This seasonal variation in IRC is reflected in the higher values observed in winter (5.06 ± 3.11 pCi/L) and fall (4.86 ± 2.92 pCi/L) compared to the lower values in summer (4.55 ± 2.84 pCi/L) and spring (3.74 ± 2.57 pCi/L) (Table S2, Figure S1). As noted in previous studies, people tend to close their windows more frequently during colder months, resulting in improved indoor enclosure and reduced gas mobility (Kellenbenz and Shakya, 2021). Additionally, the temperature difference between indoor and outdoor air can create a chimney effect, causing significant pressure differences that trap more radon gas indoors (Kellenbenz and Shakya, 2021). Conversely, the lower concentrations during warmer months are largely attributed to increased ventilation and smaller temperature differences between indoor and outdoor air. Adequate ventilation rates also help reduce other contaminants from building materials or furnishings (Zhou et al., 2022).

3.1.3 Spatial distributions

Sampling sites were primarily distributed across three large urban clusters in Ohio: Columbus (central), Cleveland (northeast), and Cincinnati (southwest). Among these, the high-IRC value sampling sites were clustered in Columbus, while the low-value sites were concentrated in Cleveland and Cincinnati (Figure 2 B1-B3). To better illustrate the spatial distribution of IRC, the results of ordinary kriging interpolation for Ohio IRC data from 2007 to 2015 are shown in Figure

S2. Overall, the spatial trend is clear, with a peak-shaped distribution, showing higher values in the center and lower values at the northeast and southwest ends along the diagonal. The southern part of Ohio borders Lake Erie, while the northern part lies along the north shore of the Ohio River. Cities in these regions are located in low-lying alluvial areas, where the soils contain more unconsolidated debris deposited by rivers and streams, resulting in lower radon levels compared to areas with granite and volcanic rocks (Briggs et al., 2008). Furthermore, Columbus contains a substantial number of aging residential buildings, many of which were constructed before radon mitigation measures were standardized in building codes. These older structures often have cracked foundations and unsealed crawl spaces or basements, providing direct pathways for radon gas to infiltrate indoor environments (Yousefian et al., 2024). Additionally, radon concentrations tend to be lower in cities than in suburban areas, as cities are often built on sedimentary rocks, which generally release less radon gas than other rock types (Darby et al., 2005). As a result, many high-IRC value sampling sites are sporadically located in suburban areas.

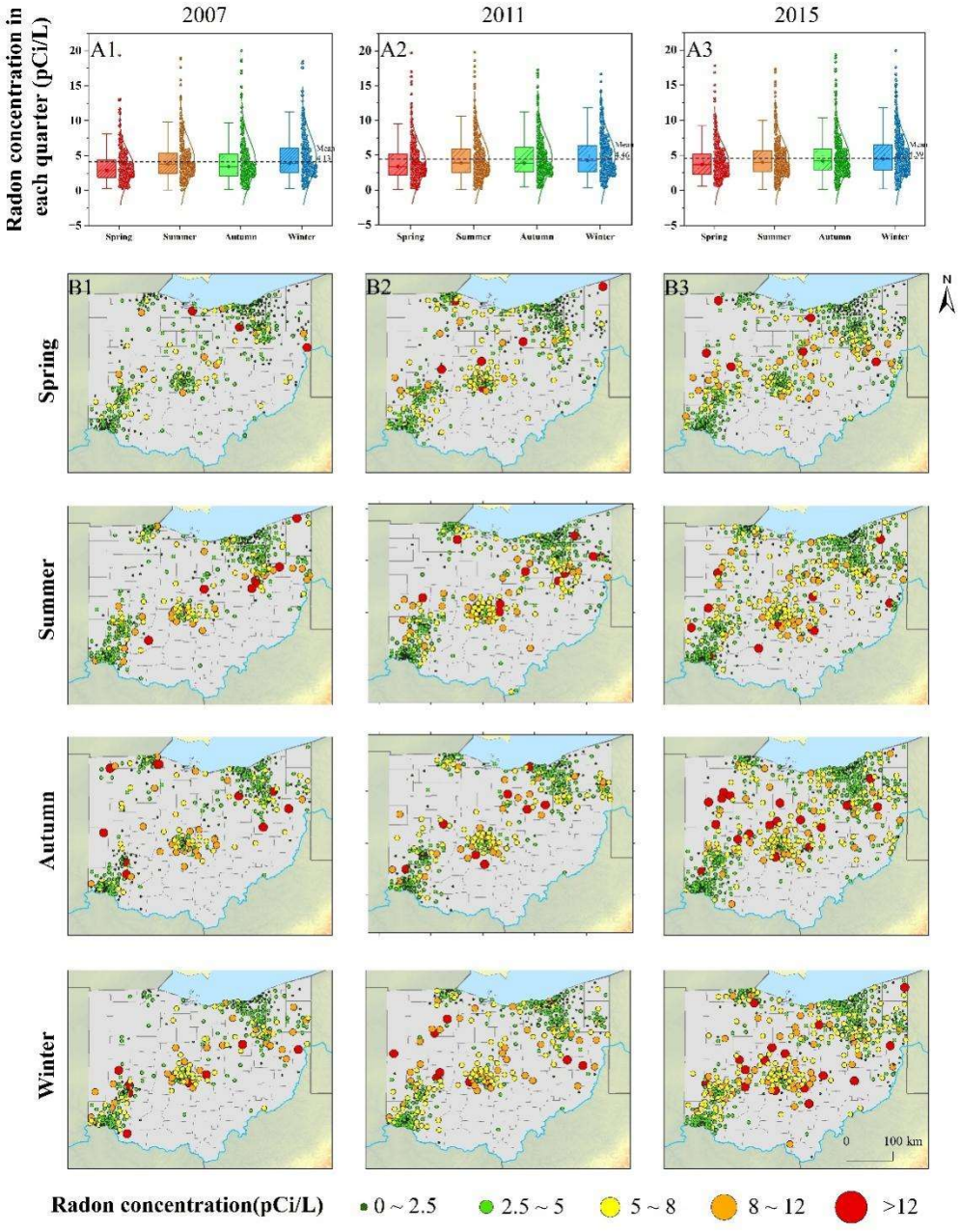

Fig. 2 (A_1-A_3) Seasonal variation of indoor radon concentration in Ohio over time. (B_1-B_3) Spatial distribution of indoor radon concentrations in different years and seasons

When we separated the IRC by building site type, we found that more developed areas had lower radon concentrations (Table S3, Figure S3). The mean IRC values for low, medium, and high development intensity areas were 4.75, 4.12, and 4.05 pCi/L, respectively. This difference in radon levels may be related to the type of housing in these areas. High-density residential areas typically consist of apartment buildings and row houses, which are more vertically oriented, leading to easier dilution of radon gas (Kellenbenz and Shakya, 2021). In contrast, medium- and low-density residential areas primarily contain single-family homes, which lack strong foundations to prevent radon infiltration and offer less room for gas dilution (Collignan et al., 2016). During poorly ventilated winter months, buildings in medium- and low-density residential areas are more likely to accumulate radon gas to unhealthy levels (Kropat et al., 2015). A previous study found that the average radon concentration in the basement of a single-story house was about twice that of a townhouse (Kellenbenz and Shakya, 2021).

3.2. Source analysis

3.2.1 Correlation analysis

Due to the varying data types of the screened environmental parameters, we employed two statistical methods to analyze their relationship with IRC. Specifically, we used Spearman correlation analysis to evaluate the impact of numerical environmental parameters on IRC distribution (Figure 3A; Table S4). Overall, uranium, thorium, soil erodibility (K factor), and organic material in the soil showed strong and significant positive effects ($r > 2$, $p < 0.001$) on indoor radon accumulation. Meanwhile, soil available water capacity and household income were also significantly positively correlated, though their effects were weaker ($1.5 < r < 2$, $p < 0.001$).

The content of uranium and thorium in the earth's crust serves as a reliable indicator for radon abundance in soil gases. Ohio, characterized by organic shale deposits with high uranium-radon concentrations, exhibits elevated levels of uranium-238, the parent element of radon, which explains the state's high radon potential (Harrell et al., 1991; Rodriguez-Martinez et al., 2018). Soil erodibility (K factor), a measure of soil's susceptibility to erosion, indicates the potential for topsoil loss under precipitation (Nguyen et al., 2023). Under conditions of higher erosion (such as sandy soils or regions susceptible to topsoil loss), thin topsoil layers are more easily disrupted or eroded by water, thereby exposing subsurface radon sources and increasing the likelihood of radon gas infiltration into buildings. Consequently, several studies have utilized the K factor as a predictor of radon concentrations (Li et al., 2021; Li et al., 2023a). The calculation of the K factor primarily considers soil texture, organic matter content, structure, and compaction (Raj et al., 2023). Stone and Hilborn (2012) reported K factor values for different soil textures and organic matter contents. For example, sandy loam soil with less than 2% organic matter had a K factor of 0.31 tonnes/hectare. This similarity in the effects of soil organic material and the K factor on IRC highlights their interconnection. Soil moisture is another crucial factor influencing indoor radon levels, as it affects radon migration and emanation. In general, soil radon data are strongly negatively correlated with soil moisture (Carrion-Matta et al., 2021; Seyis et al., 2022). Soil available water capacity (AWC), an important metric for assessing soil water retention, would theoretically exhibit a negative correlation with IRC. However, this contradicts our findings. One

possible explanation is that the relationship between AWC and IRC is complex and multifactorial, often requiring analysis within specific soil types, geological features, and climatic conditions. Previous studies have shown that precipitation has little effect on soil radon levels when the soil is saturated, as water confines radon's movement. However, the first rainfall after a prolonged dry period can lead to a sudden increase in radon levels (Seyis et al., 2022). The positive effect of household income, though initially unexpected, aligns with findings from previous studies (Casey et al., 2015; Kendall et al., 2016). Kendall et al. (2016) speculated that this might be associated with greater negative pressure in better-insulated, warmer homes, which can enhance radon infiltration.

Environmental parameters that showed a significant negative correlations with indoor radon levels included organic carbon concentration in the soil C horizon ($r = -0.16$, $p < 0.001$), snow water equivalent ($r = -0.148$, $p < 0.001$), quick-flow runoff ($r = -0.132$, $p < 0.001$), and urban impervious surfaces ($r = -0.11$, $p < 0.001$). The "C" horizon is typically the lowest layer of the soil profile, located near the bedrock, and organic carbon represents a key component of soil organic matter (e.g., plant residues, humus, etc.). Organic carbon in the soil C horizon interacts with groundwater and is linked to the presence and transport of uranium in the soil profile, which may play a role in radon dynamics (Ganguly and Bhan, 2023). Furthermore, as discussed in Section 3.1, IRC in Ohio shows significant seasonal variation and spatial heterogeneity. Some studies indicate that these seasonal variations are influenced by specific meteorological parameters. For example, low radon fluxes in winter are attributed to periodic snowmelt and ground freezing, while the decrease in radon levels during spring is likely due to increased precipitation (Fujiyoshi et al., 2006). Spatial heterogeneity is evident in the observation that building site types with more development tend to have lower radon concentrations. This suggests that building density is negatively correlated with radon levels, as areas with higher building densities typically have more impervious surfaces. Thus, snow water equivalent and urban impervious surfaces indirectly influence indoor radon levels by affecting the expulsion of radon gas from the soil. These factors may be key contributors to the spatial and temporal distribution patterns observed. Additionally, quick-flow runoff refers to water that rapidly moves through the surface, soil layers, and groundwater systems toward rivers or lakes. This phenomenon is primarily caused by intense meteorological events such as heavy rainfall or rapid snowmelt (Shi et al., 2024).

3.2.2 Risk detection analysis

Geodetector is a spatial analysis method to detect spatial heterogeneity and reveal the driving force behind it. We applied Geodetector to assess the extent to which categorical environmental parameters explained variations in indoor radon concentrations (IRC) and to determine whether significant differences existed in mean IRC values across different feature types (Figure 3 B and C). Specifically, we employed the divergence detector and factor detector to measure the explanatory power of univariate variables for spatial heterogeneity in IRC. A higher value of q indicates a stronger agreement between the variables. The top five categorical variables with the strongest explanatory power were ranked as follows: sediments ($q = 0.051$), domestic water ($q = 0.025$), sewer features ($q = 0.014$), heating fuel ($q = 0.013$), and construction materials ($q = 0.006$).

The effect of sediment type on IRC is primarily influenced by the physical properties of the sediments, their mineral composition, and factors related to the migration, accumulation, and release of radon gas. The sediment types in Ohio, covered by our sampling, include alluvial sediments, eolian sediments, glacial till sediments, glaciofluvial ice-contact sediments, and

proglacial sediments. These were further categorized based on granularity and thickness into nine subtypes. The distribution ratio of each type across sampling sites is shown in Figure S4. The results revealed that the highest IRC values were observed in areas with thick glacial till sediments, while the lowest concentrations were found in areas with fine-grained, thin proglacial sediments. Notably, all proglacial sediment types exhibited relatively low IRC. Glacial till sediments are predominantly powdery or sandy, whereas proglacial sediments consist mainly of materials deposited in glacial foreland areas due to glacial activity (Lombard et al., 2021). Kischuk et al. (2021) suggested a correlation between sediment maturity and radon gas levels. In sedimentary environments, immature sediments (e.g., glacial tills) that have undergone significant reworking show variations in grain size and sorting, which affect sediment permeability and porosity. Immature sediments with poorly sorted grain size distributions (e.g., glaciolacustrine silts) tend to have higher radon levels compared to finer-grained sediments with more uniform sorting. Furthermore, IRCs were higher in areas with a mix of relatively immature glacial till and glaciofluvial sediments than in areas dominated by more mature fluvial terrace sediments (Hansen et al., 2023).

Radon is soluble in water and can enter indoor spaces through groundwater and water supply systems. Through household activities such as bathing, drinking, and cooking, radon dissolved in water can be released into the air, contributing to indoor radon buildup (Missimer et al., 2019). According to the United Nations Scientific Committee on the Effects of Atomic Radiation (UNSCEAR) and the National Research Council, every 1000 Bq/L of radon concentration in water increases the average indoor air radon concentration by 0.1 Bq/L (UNSCEAR, 1993). Our results showed that radon levels were significantly higher in homes using private water sources (wells or springs) compared to homes with public water supplies. This finding aligns with a survey conducted in Iran, where radon concentrations in various drinking water sources were reported as follows, in descending order: tap water (2.51 Bq/L), well water (12.41 Bq/L), and spring water (153 Bq/L) (Keramati et al., 2018).

Another point worth noting is that among all building material types, the highest IRCs were found in homes with concrete, while the lowest concentrations were observed in homes with wood as the primary material. The contribution of building materials to indoor radon levels is influenced by two factors: the presence of radionuclides and the rate of radon emanation. Concrete and certain types of brick or stone can contain traces of uranium and radium, which gradually produce radon gas over time (Abujarad and Fremlin, 1983). Granite, however, is of greater concern, as it can generate an annual effective dose that exceeds the European regulation's recommended exposure limit of 1 mSv/y. It also has a higher radon emission rate (42 Bq $m^{-2}d^{-1}$) compared to renovation materials like slate (30 Bq $m^{-2}d^{-1}$) (Ajrouche et al., 2017). Fortunately, none of the homes in our sampling area used granite-based building materials. In contrast, homes primarily constructed with wood generally had low indoor radon levels. This is likely due to the fact that wooden structures typically have deep cavities, which facilitate the natural penetration and escape of indoor radon gas (Yazzie et al., 2020).

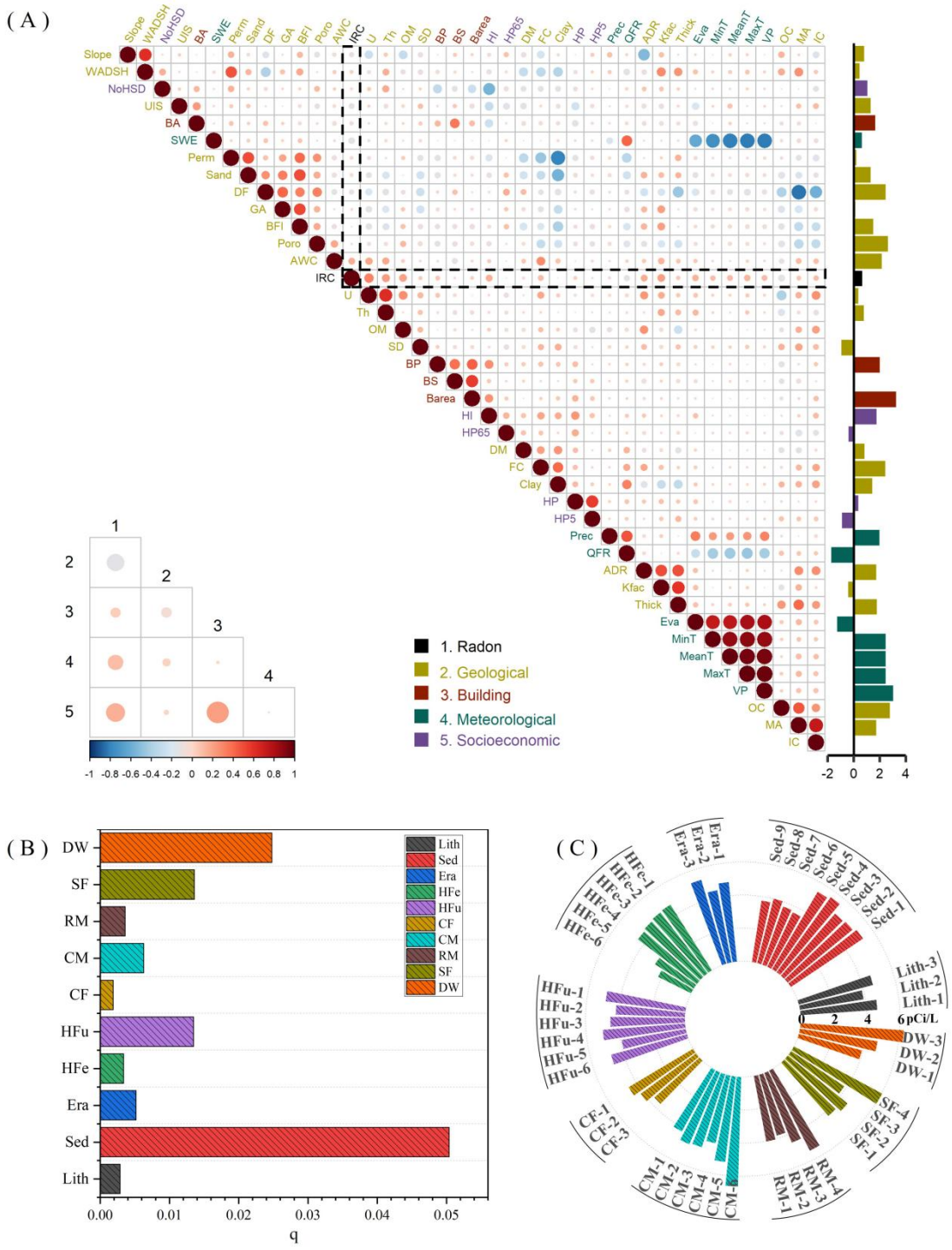

Fig. 3. (A) Correlations between IRC and numerical environmental factors, as well as between different subgroups, with horizontal bars representing the distribution of log10-transformed data for each group. (B) Explanatory power of categorical environmental factors for IRC (results of factor detection analysis). (C) Mean IRC in different subregions based on categorical environmental factors (results of risk detection)

3.2.3 Structural equation model analysis

Since the effects of individual environmental factors exhibit similar enrichment characteristics and fail to capture the direct, indirect, and combined effects of different variables on IRC, we employed PLS-SEM to estimate the causal relationships between multiple dependent

and independent variables (Figure 4). The latent variables were grouped into fifteen categories: geological tectonics, geophysical features, soil composition, soil water, soil characteristics, surface features, surface radiation, hydroclimate, building features, building materials, heating features, cooling features, domestic water, socioeconomic factors, and population. The model was analyzed by combining correlation analysis with GOF to optimize and adjust it. A total of 35 environmental indicators were recombined as latent variables, and the relationships between all observed and latent variables are presented in Table S5. Sensitivity tests for the path coefficients were performed via the bootstrap function with 5000 samples. Table S6 presents a summary of the path results along with the corresponding t-values and the estimated p-values associated with each t-value. Overall, surface radiation had a major positive contribution to IRC, while building materials and hydroclimate had major negative contributions. Additionally, hydroclimate exerted a greater direct effect than an indirect effect on IRC, whereas geological tectonics, soil features, building features, and socioeconomic factors had stronger indirect than direct effects.

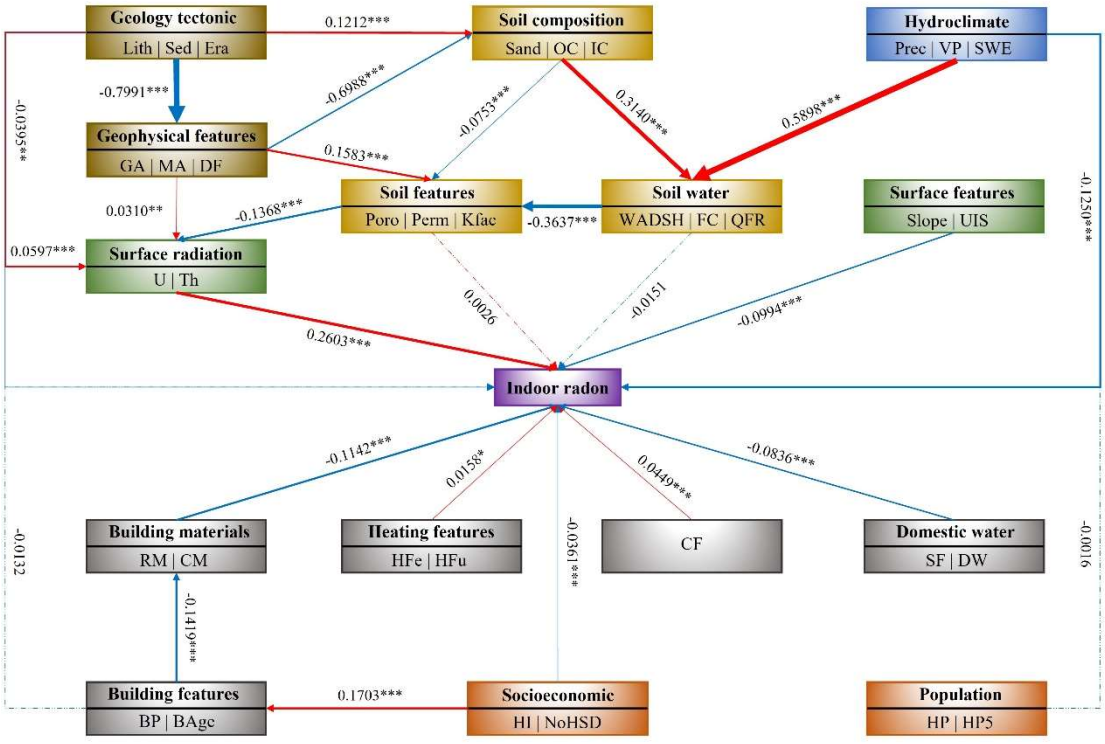

Fig. 4. PLS-SEM showing the direct and indirect effects of environmental parameters on IRC. The sample GOF value is 0.4009. Red and blue arrows represent positive and negative effects, respectively, with the arrow width proportional to the effect strength. *: $p < 0.05$, **: $p < 0.01$, and ***: $p < 0.001$. Solid lines indicate significant relationships, while dashed lines indicate non-significant relationships

Structural equation modeling effectively captures multiple dependencies and complex causal structures. Using this model, we quantitatively explain the internal logic behind the effects of geological composition (lithology, sedimentation, and geological age) on IRC. Specifically, different types of sediments and rocks contain varying levels of radionuclides (e.g., uranium or thorium), leading to differences in the original crustal radon gas produced through their decomposition. This relationship is also evident in soil features, which influence the transport and migration capacity of radon in the soil (Li et al., 2023a). The model also revealed several intriguing

findings. For example, while building features (e.g., building age and building price) and socioeconomic factors (e.g., household income and the proportion of individuals aged 25^{+} without a high school diploma) have insignificant or weak direct effects on IRC, they can indirectly influence radon levels through their impact on building materials. Building age, for instance, reflects the aging of materials, which over time release more airborne radioactivity and are prone to deterioration, cracking, and settling. These cracks provide pathways for radon gas to infiltrate indoors (Li et al., 2023a).

3.3. Radon exposure health risk assessment

Based on the radon effective dose calculation method and two risk assessment models, we calculated the E_{Rn}, LCC, and ELCR for indoor radon in Ohio, taking into account population risk factors. The Kriging interpolation of risk values around the sampling points is shown in Figure 5 (A, B). The overall mean annual effective radiation dose for household radon exposure in Ohio was 4.19 mSv/y, which is higher than the global average of 1.3 mSv/y (Radiation, 2011), even most households are exposed within the range of workplace action levels specified by the ICRP (3–10 mSv/y) (Valentin, 2007). The mean LCC value was 86.14 per million people. While this is lower than the ICRP recommended range of 170–230 per million (Valentin, 2007), it is significantly higher than similar studies conducted in Iran (32.62 per million) (Azhdarpoor et al., 2021), Italy (2.1 per million) (Loffredo et al., 2021), and China (29.5 per million) (Lin et al., 2024). Additionally, after adjusting for age, gender, and smoking status, the overall mean ELCR was 2.29%, which is higher than the U.S. EPA action level of 1.3% (Azhdarpoor et al., 2021). Overall, long-term exposure to radon and its daughters poses a significant health risk to Ohio occupants and workers.

Spatially, high-risk areas are concentrated in central Ohio, with risk values decreasing from the central region to the surrounding cities. The major high-risk city is Columbus, a second-high-risk city is Canton, and the three major low-risk cities are Cincinnati in the Southwest and Cleveland and Parma in the Northeast. The primary reason for this spatial distribution pattern is the variation in IRC (Figure S2), with a secondary factor being the population's ability to mitigate the risk of radon exposure (Figure S5). Higher risks were observed in areas with high IRC, a larger proportion of elderly populations, a higher proportion of male populations, and a higher prevalence of smoking.

Monte Carlo simulation results showed that radon exposure risk was moderate for all groups, with mean ELCR values of 1.38, 1.72, 2.24, 1.72, 2.06, 1.71, and 2.58 for minors, adults, the elderly, females, males, smokers, and non-smokers, respectively (Figure 5C). The highest exposure risk was observed in the elderly age group, with a risk 1.3 and 1.62 times higher than for adults and minors, respectively. Due to limitations in energy and mobility, elderly individuals spend most of their time at home or in retirement centers, resulting in higher exposure to radon (Lee et al., 2024). Furthermore, as people age, their physiological ability to regulate and compensate for the effects of pollutant exposure diminishes (Guo et al., 2016). The risk for smokers was significantly higher than that of non-smokers. Both residential radon studies and miners' studies have shown that the absolute risk of lung cancer from radon is much lower in never-smokers than in smokers or ex-smokers (Madas et al., 2022). Evidence overwhelmingly supports that the combined effect of radon and smoking on lung cancer is submultiplicative (between additive and multiplicative) (Su et al., 2022b). One explanation for this is that radon and

tobacco smoke act as co-carcinogens. Smoking can impair lung function, increasing the accumulation of radon in lung tissue and intensifying its radiant energy (Riudavets et al., 2022). In contrast, potential gender-specific susceptibility to radon-induced cancer may be attributed to differences in smoking prevalence, biological factors, and exposure patterns (Kalankesh et al., 2024).

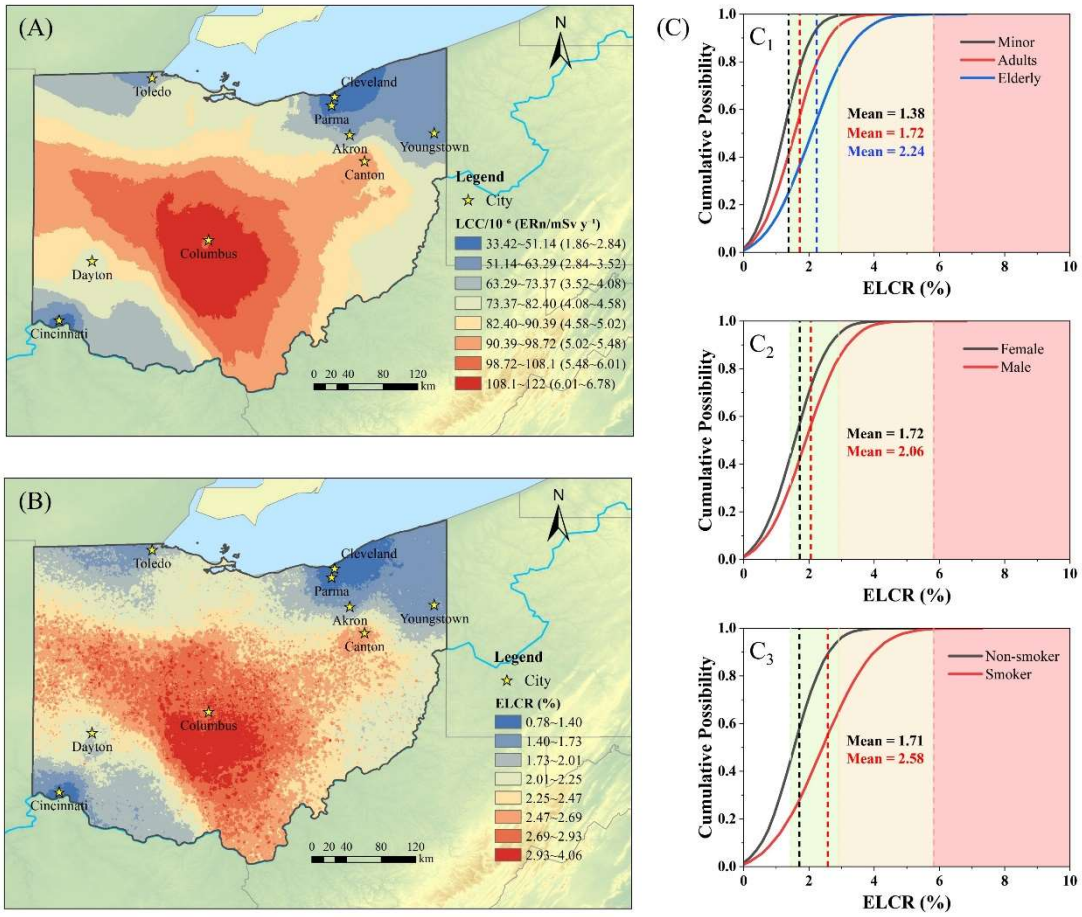

Fig. 5: (A) Spatial distribution of LCC and E_{Rn}, with overall mean values of 86.14 per million population and 4.79 mSv/y, respectively. (B) Spatial distribution of ELCR (considering demographic risk factors), with an overall mean value of 2.29%. (C) Probability distribution of excess lifetime cancer risk due to radon exposure (C_1: age group; C_2: gender group; C_3: smoking status group). The white, green, yellow, and red areas represent low, moderate, considerable, and very high risk, respectively. The boundary values correspond to the excess lifetime cancer risk at radon concentrations of 148 Bq/m³, 300 Bq/m³, and 600 Bq/m³, respectively

4. Conclusion

This study systematically investigated the spatial and temporal variability of indoor radon levels, their sources, and associated health risks in Ohio using multi-source geographic data. The annual mean indoor radon concentrations ranged from 4.13 to 5.03 pCi/L, with an overall mean effective radiation dose of 4.79 mSv/y, approximately 3.68 times the global average (1.3 mSv/y). Spatially, high radon concentrations were clustered in Columbus and decreased from the central urban agglomeration to surrounding areas. Additionally, more developed building site types exhibited lower IRC. Temporally, IRC demonstrated an increasing trend, with distinct seasonal

variations characterized by higher concentrations in winter compared to summer. Key influencing factors included radiation sources, such as uranium and thorium at the Earth's surface, followed by meteorological conditions and housing materials. Human activities, such as heating methods and water use, also correlated strongly with IRCs, with lower values observed in homes utilizing public water systems and open heating methods. Unexpectedly, economically disadvantaged households exhibited lower indoor radon levels than wealthier households, potentially due to structural differences or lower insulation quality, rather than greater awareness or mitigation practices. This discrepancy is concerning, as radon exposure in Ohio poses a significant health risk, with an overall excess lifetime cancer risk averaging 2.29%, nearly double the U.S. EPA's action level of 1.3%. These findings underscore the urgent need for enhanced radon monitoring, increased public awareness, and effective mitigation strategies. Future efforts should prioritize the collection of updated radon testing data, the implementation of long-term monitoring programs, and the integration of multi-source impact mechanisms and risk assessment frameworks to inform policy development and public health protection. Although this study successfully identifies key influencing factors and delineates high-risk areas, the precise detection and effective removal of radon sources require detailed, site-specific investigations that consider geological and structural complexities. Bridging the gap between large-scale risk modeling and localized mitigation strategies should be a major focus of future research aimed at advancing radon source control and health risk reduction.

References

Abujarad, F., Fremlin, J.H., 1983. EFFECT OF INTERNAL WALL COVERS ON RADON EMANATION INSIDE HOUSES. Health Physics 44, 243-248.

Acree, P., Puckett, M., Neri, A., 2017. Evaluating progress in radon control activities for lung cancer prevention in national comprehensive cancer control program plans, 2011–2015. Journal of community health 42, 962-967.

Ajrouche, R., Ielsch, G., Clero, E., Roudier, C., Gay, D., Guillevic, J., Laurier, D., Le Tertre, A., 2017. Quantitative Health Risk Assessment of Indoor Radon: A Systematic Review. Radiation Protection Dosimetry 177, 69-77.

Azhdarpoor, A., Hoseini, M., Shahsavani, S., Shamsedini, N., Gharehchahi, E., 2021. Assessment of excess lifetime cancer risk and risk of lung cancer due to exposure to radon in a middle eastern city in Iran. Radiation Medicine and Protection 2, 112-116.

Briggs, D., Abellan, J.J., Fecht, D., 2008. Environmental inequity in England: Small area associations between socio-economic status and environmental pollution. Social Science & Medicine 67, 1612-1629.

Bulut, H.A., Sahin, R., 2023. Activity concentration and annual effective dose assessments of radon in SCCs with different mineral additives. Construction and Building Materials 364.

Carrion-Matta, A., Lawrence, J., Kang, C.-M., Wolfson, J.M., Li, L., Vieira, C.L.Z., Schwartz, J., Demokritou, P., Koutrakis, P., 2021. Predictors of indoor radon levels in the Midwest United States. Journal of the Air & Waste Management Association 71, 1515-1528.

Casey, J.A., Ogburn, E.L., Rasmussen, S.G., Irving, J.K., Pollak, J., Locke, P.A., Schwartz, B.S., 2015. Predictors of Indoor Radon Concentrations in Pennsylvania, 1989-2013. Environmental Health Perspectives 123, 1130-1137.

Chaudhuri, H., Das, N.K., Bhandari, R.K., Sen, P., Sinha, B., 2010. Radon activity measurements around Bakreswar thermal springs. Radiation Measurements 45, 143-146.

Chen, L., Yao, Y., Xiang, K., Dai, X., Li, W., Dai, H., Lu, K., Li, W., Lu, H., Zhang, Y., 2024. Spatial-temporal pattern of ecosystem services and sustainable development in representative mountainous cities: A case study of Chengdu-Chongqing Urban Agglomeration. Journal of Environmental Management 368, 122261.

Chen, M.S., Bill, D., 1983. STATEWIDE SURVEY OF RISK FACTOR PREVALENCE - THE OHIO EXPERIENCE. Public Health Reports 98, 443-448.

Collignan, B., Le Ponner, E., Mandin, C., 2016. Relationships between indoor radon concentrations, thermal retrofit and dwelling characteristics. Journal of Environmental Radioactivity 165, 124-130.

Darby, S., Hill, D., Auvinen, A., Barrios-Dios, J.M., Baysson, H., Bochicchio, F., Deo, H., Falk, R., Forastiere, F., Hakama, M., Heid, I., Kreienbrock, L., Kreuzer, M., Lagarde, F., Mäkeläinen, I., Muirhead, C., Oberaigner, W., Pershagen, G., Ruano-Ravina, A., Ruosteenoja, E., Rosario, A.S., Tirmarche, M., Tomásek, L., Whitley, E., Wichmann, H.E., Doll, R., 2005. Radon in homes and risk of lung cancer:: collaborative analysis of individual data from 13 European case-control studies. Bmj-British Medical Journal 330, 223-226.

Deinpsey, S., Lyons, S., Nolan, A., 2018. High Radon Areas and lung cancer prevalence: Evidence from Ireland. Journal of Environmental Radioactivity 182, 12-19.

Forouzanfar, M.H., Alexander, L., Anderson, H.R., al, e., 2015. Global, regional, and national comparative risk assessment of 79 behavioural, environmental and occupational, and metabolic risks or clusters of risks in 188 countries, 1990-2013: a systematic analysis for the Global Burden of Disease Study 2013. Lancet 386, 2287-2323.

Fujiyoshi, R., Sakamoto, K., Imanishi, T., Sumiyoshi, T., Sawamura, S., Vaupotic, J., Kobal, I., 2006. Meteorological parameters contributing to variability in ²²²Rn activity concentration's in soil gas at a site in Sapporo, Japan. Science of the Total Environment 370, 224-234.

Ganguly, S., Bhan, U., 2023. Occurrences and mobility of uranium in soil profile due to groundwater–soil interaction. Hydrogeochemistry of Aquatic Ecosystems, 181-198.

Gu, X., Lin, C., Liu, Z., Chu, Z., Ouyang, W., He, M., Liu, X., 2022. Heavy metal distribution in Chinese coastal sediments and organisms: Human impacts, probabilistic risks and sensitivity analysis. Journal of Hazardous Materials Advances 7, 100147.

Gummadi, J., Bhatt, D., Adusumilli, S., Devabhaktuni, V., Acosta, W., Kumar, A., 2015. Interpolation techniques for modeling and estimating indoor radon concentrations in Ohio: Comparative study. Environmental Progress & Sustainable Energy 34, 169-177.

Guo, L., Li, H., Cao, X., Cao, A., Huang, M., 2021. Effect of agricultural subsidies on the use of chemical fertilizer. Journal of Environmental Management 299, 113621.

Guo, Y., Zeng, H., Zheng, R., Li, S., Barnett, A.G., Zhang, S., Zou, X., Huxley, R., Chen, W., Williams, G., 2016. The association between lung cancer incidence and ambient air pollution in China: A spatiotemporal analysis. Environmental Research 144, 60-65.

Hahn, E.J., Wilmhoff, C., Rayens, M.K., Conley, N.B., Morris, E., Larck, A., Allen, T., Pinney, S.M., 2020. High school students as citizen scientists to decrease radon exposure. International Journal of Environmental Research and Public Health 17, 9178.

Hansen, V., Sabo, A., Korn, J., MacLean, D., Riget, F.F., Clausen, D.S., Cubley, J., 2023. Indoor radon survey in Whitehorse, Canada, and dose assessment. Journal of Radiological Protection 43.

Harrell, J.A., Belsito, M.E., Kumar, A., 1991. RADON HAZARDS ASSOCIATED WITH OUTCROPS OF OHIO SHALE IN OHIO. Environmental Geology and Water Sciences 18, 17-26.

Kalankesh, L.R., Mosaferi, M., Khajavian, N., Sarvari, B., Zarei, A., 2024. Simulation excess lifetime lung cancer risk due to indoor radon exposure in Eastern Iran - Monte Carlo Simulation method. Journal of Radiation Research and Applied Sciences 17.

Kellenbenz, K.R., Shakya, K.M., 2021. Spatial and temporal variations in indoor radon concentrations in Pennsylvania, USA from 1988 to 2018. Journal of Environmental Radioactivity 233.

Kendall, G.M., Miles, J.C.H., Rees, D., Wakeford, R., Bunch, K.J., Vincent, T.J., Little, M.P., 2016. Variation with socioeconomic status of indoor radon levels in Great Britain: The less affluent have less radon. Journal of Environmental Radioactivity 164, 84-90.

Keramati, H., Ghorbani, R., Fakhri, Y., Khaneghah, A.M., Conti, G.O., Ferrante, M., Ghaderpoori, M., Taghavi, M., Baninameh, Z., Bay, A., Golaki, M., Moradi, B., 2018. Radon 222 in drinking water resources of Iran: A systematic review, meta-analysis and probabilistic risk assessment (Monte Carlo simulation). Food and Chemical Toxicology 115, 460-469.

Kim, J., Kaown, D., Lee, K.-K., 2024. Coupling of radon and microbial analysis for dense non-aqueous-phase liquid tracing and health risk assessment in groundwater under seasonal variations. Journal of Hazardous Materials 475.

Kishchuk, M.J., Lipovsky, P.S., Bond, J.D., Gosse, J.C., 2021. Investigation of geological controls on radon concentration in surficial sediment in Whitehorse, Yukon, Canada. Atlantic Geology 57, 119-121.

Kropat, G., Bochud, F., Jaboyedoff, M., Laedermann, J.-P., Murith, C., Palacios, M., Baechler, S., 2015. Predictive analysis and mapping of indoor radon concentrations in a complex environment using kernel estimation: An application to Switzerland. Science of the Total Environment 505, 137-148.

Kumar, A., Kadiyala, A., Devabhaktuni, V., Akkala, A., Manthena, D.V., 2010. Examination of Ohio indoor radon data, American Association of Radon Scientists and Technologists (AARST) Proceedings of 22 nd International Radon Symposium. Columbus, OH. Citeseer.

Kumar, A., Varadarajan, C., Kadiyala, A., 2011. Management of radon data in the state of Ohio, USA. Open Environ Biol Monitor J 4, 57-71.

Lecomte, J.F., Solomon, S., Takala, J., Jung, T., Strand, P., Murith, C., Kiselev, S., Zhuo, W., Shannoun, F., Janssens, A., International Commission on Radiological, P., 2014. ICRP Publication 126: Radiological Protection against Radon Exposure. Annals of the ICRP 43, 5-73.

Lee, S.-Y., Lim, S.-H., Kim, H.-S., 2024. Assessing the Radon Exposure Variability and Lifetime Health Effects across Indoor Microenvironments and Sub-Populations. Atmosphere 15.

Li, L., Blomberg, A.J., Stern, R.A., Kang, C.-M., Papatheodorou, S., Wei, Y., Liu, M., Peralta, A.A., Vieira, C.L.Z., Koutrakis, P., 2021. Predicting Monthly Community-Level Domestic Radon Concentrations in the Greater Boston Area with an Ensemble Learning Model. Environmental Science & Technology 55, 7157-7166.

Li, L., Stern, R.A., Garshick, E., Zilli Vieira, C.L., Coull, B., Koutrakis, P., 2023a. Predicting Monthly Community-Level Radon Concentrations with Spatial Random Forest in the Northeastern and Midwestern United States. Environmental Science & Technology.

Li, L., Stern, R.A., Garshick, E., Zilli Vieira, C.L., Coull, B., Koutrakis, P., 2023b. Predicting monthly community-level radon concentrations with spatial random forest in the Northeastern and Midwestern United States. Environmental science & technology 57, 18001-18012.

Lin, C.-C., Lin, S.-J., Li, P.-Y., Lee, M.S., Ting, C.-Y., 2024. Radon levels and dose assessment at

the basement workplaces of hospitals in different regions of Taiwan. Radiation Physics and Chemistry 218.

Liu, C., Chen, J., Zhang, W., Ungar, K., 2024a. Outdoor Radon Dose Rate in Canada's Arctic amid Climate Change. Environmental Science & Technology 58, 11309-11319.

Liu, Y., Xu, Y., Li, Y., Wei, H., 2023. Identifying the environmental determinants of lung cancer: A case study of Henan, China. GeoHealth 7, e2023GH000794.

Liu, Y., Xu, Y., Xu, W., He, Z., Fu, C., Du, F., 2024b. Radon and lung cancer: Current status and future prospects. Critical Reviews in Oncology Hematology 198.

Loffredo, F., Savino, F., Amato, R., Irollo, A., Gargiulo, F., Sabatino, G., Serra, M., Quarto, M., 2021. Indoor Radon Concentration and Risk Assessment in 27 Districts of a Public Healthcare Company in Naples, South Italy. Life-Basel 11.

Lombard, M.A., Bryan, M.S., Jones, D.K., Bulka, C., Bradley, P.M., Backer, L.C., Focazio, M.J., Silverman, D.T., Toccalino, P., Argos, M., Gribble, M.O., Ayotte, J.D., 2021. Machine Learning Models of Arsenic in Private Wells Throughout the Conterminous United States As a Tool for Exposure Assessment in Human Health Studies. Environmental Science & Technology 55, 5012-5023.

Madas, B.G., Boei, J., Fenske, N., Hofmann, W., Mezquita, L., 2022. Effects of spatial variation in dose delivery: what can we learn from radon-related lung cancer studies? Radiation and Environmental Biophysics 61, 561-577.

Manawi, Y., Hassan, A., Atieh, M.A., Lawler, J., 2024. Overview of radon gas in groundwater around the world: Health effects and treatment technologies. Journal of environmental management 368, 122176.

Missimer, T.M., Teaf, C., Maliva, R.G., Danley-Thomson, A., Covert, D., Hegy, M., 2019. Natural Radiation in the Rocks, Soils, and Groundwater of Southern Florida with a Discussion on Potential Health Impacts. International Journal of Environmental Research and Public Health 16.

Nayak, T., Basak, S., Deb, A., Dhal, P.K., 2022. A systematic review on groundwater radon distribution with human health consequences and probable mitigation strategy. Journal of Environmental Radioactivity 247.

Nguyen, V.T., Huynh, N.P.T., Huynh, T.Y.H., Truong, H.N.T., Le, B.A., Huynh, T.P., Le, C.H., 2023. Effects of soil erosion on natural radioactivity in water in a typical quarry lake in Vietnam based on model assessment. Journal of Radioanalytical and Nuclear Chemistry 332, 2359-2366.

Parveen, N., Siddiqui, L., Sarif, M.N., Islam, M.S., Khanam, N., Mohibul, S., 2021. Industries in Delhi: Air pollution versus respiratory morbidities. Process Safety and Environmental Protection 152, 495-512.

Poku, B., Hussaini, S., 2024. Assessing State Laws and Regulations on Radon in US Childcare Centers. Journal of Global Awareness 5, 1-24.

Radiation, U.N.S.C.o.t.E.o.A., 2011. Sources and Effects of Ionizing Radiation: Report to the General Assembly with Scientific Annexes. Volume 2. Annex D. Health Effects Due to Radiation from the Chernobyl Accident.(advanced Copy). UN.

Raj, R., Saharia, M., Chakma, S., 2023. Mapping soil erodibility over India. Catena 230.

Riudavets, M., Garcia de Herreros, M., Besse, B., Mezquita, L., 2022. Radon and Lung Cancer: Current Trends and Future Perspectives. Cancers 14.

Robertson, A., Allen, J., Laney, R., Curnow, A., 2013. The Cellular and Molecular Carcinogenic Effects of Radon Exposure: A Review. International Journal of Molecular Sciences 14, 14024-14063.

Rodriguez-Martinez, A., Torres-Duran, M., Barros-Dios, J.M., Ruano-Ravina, A., 2018.

Residential radon and small cell lung cancer. A systematic review. Cancer Letters 426, 57-62.

Schubert, M., Musolff, A., Weiss, H., 2018. Influences of meteorological parameters on indoor radon concentrations (²²²Rn) excluding the effects of forced ventilation and radon exhalation from soil and building materials. Journal of Environmental Radioactivity 192, 81-85.

Seyis, C., Inan, S., Yalcin, M.N., 2022. Major factors affecting soil radon emanation. Natural Hazards 114, 2139-2162.

Shi, X., Zheng, Y., Su, J., Zhang, F., Zhu, J., Zeng, C., 2024. Spatiotemporal refinement of hydro-sediment processes in small disturbed permafrost watershed during rainfall and snowmelt events. Catena 247.

Smith, H., 1988. Lung cancer risk from indoor exposure to radon daughters. Radiology 167, 580-580.

Somsunun, K., Prapamontol, T., Pothirat, C., Liwsrisakun, C., Pongnikorn, D., Fongmoon, D., Chantara, S., Wongpoomchai, R., Naksen, W., Autsavapromporn, N., Tokonami, S., 2022. Estimation of lung cancer deaths attributable to indoor radon exposure in upper northern Thailand. Scientific Reports 12.

Stone, R., Hilborn, D., 2012. Universal soil loss equation (USLE) factsheet. Ministry of Agriculture, Food and Rural Affairs order.

Su, C., Pan, M., Liu, N., Zhang, Y., Kan, H., Zhao, Z., Deng, F., Zhao, B., Qian, H., Zeng, X., Sun, Y., Liu, W., Mo, J., Guo, J., Zheng, X., Sun, C., Zou, Z., Li, H., Huang, C., 2022a. Lung cancer as adverse health effect by indoor radon exposure in China from 2000 to 2020: A systematic review and meta-analysis. Indoor Air 32.

Su, Z., Wei, M.-N., Jia, X.-H., Fan, Y.-G., Zhao, F.-H., Zhou, Q.-H., Taylor, P.R., Qiao, Y.-L., 2022b. Arsenic, tobacco use, and lung cancer: An occupational cohort with 27 follow-up years. Environmental Research 206.

Takahashi, L.C., Santos, T.d.O., Marques Pinheiro, R.M., Passos, R.G., Rocha, Z., 2022. Radon dosimetry using Solid State Nuclear Track Detectors in different environments: a review. Applied Radiation and Isotopes 186.

Tung, S., Leung, J.K.C., Jiao, J.J., Wiegand, J., Wartenberg, W., 2013. Assessment of soil radon potential in Hong Kong, China, using a 10-point evaluation system. Environmental Earth Sciences 68, 679-689.

Turner, M.C., Krewski, D., Chen, Y., Pope, C.A., III, Gapstur, S., Thun, M.J., 2011. Radon and Lung Cancer in the American Cancer Society Cohort. Cancer Epidemiology Biomarkers & Prevention 20, 438-448.

UNSCEAR, S., 1993. Effects of ionizing radiation, United Nations Scientific Committee on the Effects of Atomic Radiation, Report to the General Assembly, with Scientific Annexes, United Nations Publication sales No. E 00 IX 3.

Valentin, J., 2007. International Commission on Radiological Protection. The 2007 recommendations of the international commission on radiological protection. Annals of the ICRP, ICRP Publication 103, 2-4.

Wan, T., Shi, B., 2022. Exploring the interactive associations between urban built environment features and the distribution of offender residences with a geodetector model. ISPRS International Journal of Geo-Information 11, 369.

Wang, J.-F., Zhang, T.-L., Fu, B.-J., 2016. A measure of spatial stratified heterogeneity. Ecological indicators 67, 250-256.

Xie, D., Liao, M., Kearfott, K.J., 2015. Influence of environmental factors on indoor radon concentration levels in the basement and ground floor of a building - A case study. Radiation Measurements 82, 52-58.

Xie, J., Tao, L., Wu, Q., Bian, Z., Wang, M., Li, Y., Zhu, G., Lin, T., 2022. Bioaccumulation of organochlorine pesticides in Antarctic krill (Euphausia superba): Profile, influencing factors, and mechanisms. Journal of Hazardous Materials 426, 128115.

Xue, Y., Wang, L., Zhang, Y., Zhao, Y., Liu, Y., 2022. Air pollution: A culprit of lung cancer. Journal of Hazardous Materials 434.

Yazzie, S.A., Davis, S., Seixas, N., Yost, M.G., 2020. Assessing the Impact of Housing Features and Environmental Factors on Home Indoor Radon Concentration Levels on the Navajo Nation. International Journal of Environmental Research and Public Health 17.

Yousefian, F., Nasiri, Z., Kordi, M., Marzi, Y.G., Dehghani, R., Mirzaei, N., Janjani, H., Aghaei, M., Aboosaedi, Z., 2024. Indoor Radon and Its Health Risk Assessment in Iran: A Comprehensive Review Study. Indoor Air 2024, 2300116.

Zhou, J.R., Zheng, R., Tang, J., Sun, H.J., Wang, J., 2022. A mini-review on building insulation materials from perspective of plastic pollution: Current issues and natural fibres as a possible solution. Journal of Hazardous Materials 438.